4D Dual-V_{enc} Spiral Flow

Sean Callahan[1], Alex Henn[1], Michael Kendrick[2], Hui Wang[5], MJ Negahdar[1], Arash Kheradvar[4], Marcus Stoddard[23], and Amir Amini[1] *IEEE Fellow*
[1]*Medical Imaging Lab, Department of Electrical and Computer Engineering &*
[2]*Division of Cardiovascular Medicine, University of Louisville*
[3]*Robley Rex Veterans Affairs Medical Center, Louisville, KY*
[4]*Edwards Lifesciences Center, University of California, Irvine*
[5]*Philips, Gainesville, FL*

***Abstract*— Dual-Venc flow acquisition sequences perform flow imaging with differing Vencs. The technique can be used to improve velocity to noise ratio and image quality for diastolic flow velocities as part of a single scan. In this paper, Dual-Venc was used in conjunction with spiral read-out trajectories, offering a faster coverage of k-space. The results illustrate that 4D Dual Venc Spiral Flow behaves similarly to 4D Dual-Venc Cartesian Flow but with the benefit of faster acquisition time and lower echo time (TE).**

I. Introduction

4D Flow imaging is an MRI based method that permits direct measurement of a target region's flow rate while allowing exquisite visualization of flow. This is done via phase-contrast (PC) MRI velocity encoding amplifying the 1st gradient moment, and nulling the 0th moment. The difference between the conventional PC and 4D Flow is the spatial/k-space dimension of the acquisition. PC acquisitions, clinically implemented, capture flow through a defined plane, whilst 4D Flow captures flow throughout a 3D region. PC imaging is therefore faster, but is prone to misplacement due to either user error, or unknown aspects of the flow – for example when the plane is not orthogonal to the major velocity direction, causing foreshortening and resulting in under estimation of the actual flow velocity. With 4D flow, there is less concern about slice misplacement, as all voxels within the region will be acquired, but this is at the cost of longer scan times and acquisition of more data. Long scan times can lead to patient discomfort, requiring sacrificing imaging fidelity to reach acceptable scan times [1].

Scan time reduction for 4D Flow is an active area of research. There are many methods that can be used to shorten the 4D Flow sequence scan time most of which rely upon some form of redundancy in k-space in either the spatial, temporal or spatial and temporal dimensions. Examples of these techniques are k-t BLAST, k-t GRAPPA, and k-t SENSE [2] [3]. A related technique compressive sensing – requires undersampling of k-space relying upon minimizing the reconstruction artifacts, by sampling pseudo-randomly [4]. These techniques are most often implemented for a Cartesian readout trajectory. In addition to k-space undersampling strategies, non-Cartesian trajectories may offer improved scan efficiency as well. These trajectories involve radial or spiral readouts and achieve a shorter TE, which improve flow image quality in reducing phase incoherence [5], [6]. If ϕ represents phase information, velocity for a given direction, $V = \frac{\varphi}{\pi} * \text{Venc}$, where Venc is a user-specified parameter which typically is set to the highest velocity in the flow corresponding to a phase shift of π. Setting Venc below the highest velocity will lead to phase wrap and velocity aliasing. Dual-Venc is a flow imaging strategy which allows for the acquisition of flow data at different Vencs. This approach improves velocity resolution in the low flow phases of the cardiac cycle while adapting to higher velocities at higher flow rates in order to avoid aliasing. In the cardiovascular system, peak velocities can approximately reach 400-600 cm/s in systole, and below 50 cm/s in diastole – a single Venc strategy that avoids velocity aliasing therefore would be prone to loss of velocity resolution at low flow rates. Additionally, it is known that SNR is inversely proportional to Venc. Therefore a lower Venc is generally desirable [7]. Dual-Venc strategies are implemented via multiple scans, stitching the flow data together [8], using a single flow encoding sequence to acquire the images for all the desired Vencs at all time points, or using single sequence with a temporally variant Venc. The Dual-Venc sequence, which is only one scan, and acquires images for each Venc has the advantage of total scan time savings over acquiring with different Venc via separate scans as seen in [9]. The other scan, which varies Venc temporally, loses the redundant low Venc information that can be gained via multiple images of the same location at differing Venc, but has the scan time of a single Venc scan, and targets the Venc to the system.

In order to perform 4D flow imaging, we propose a temporal based Dual-Venc strategy, with Spiral readouts – this achieves good velocity resolution and velocity noise resolution (VNR) in diastole as well as good scan efficiency. The sequence has been applied to phantoms, as well as valvular flows through the aortic valve of healthy volunteers and compared with the conventional Cartesian readout.

II. Methodology

A. Pulse Sequence

This paper is centered on a temporally variant 4D Dual-Venc Spiral Flow sequence. The method starts with the lowest Venc and optimizes around this scan. Once the low Venc scan is optimized, the bipolar gradient strength is relaxed to match the higher Venc. This allows the TE to be consistent for the extent of the scan, which maintains the TR and temporal resolution. The temporal variation in Venc was

978-1-5386-3646-6/18/$31.00 ©2018 IEEE

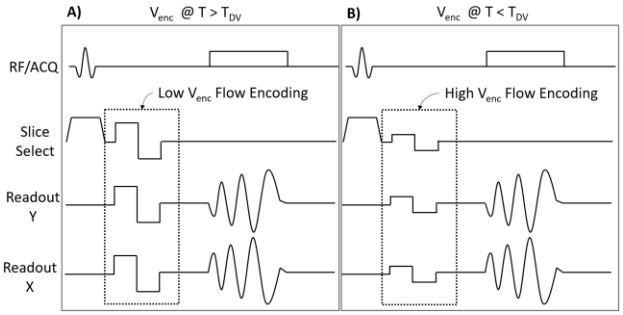

Figure 1: The first acquisition in a 4 point Hadamard Spiral pulse sequence. A) is a low Venc acquisition, which occurs after T_{DV}, while B) is a high Venc acquisition that occurs before T_{DV}. These acquisitions have the same TE, and TR, and occur at different times in the cardiac cycle.

prescribed to take advantage of the difference between systolic and diastolic velocities, and can be seen in Figure 1.

B. Phantoms

A flow phantom with a valvular inclusion was scanned. The valvular phantom's imaging area is a clear axisymmetric plexiglass housing that allows for easy exchange of the synthetic valves with different orifice areas. The inlet end contains a lip that the 25.4 mm diameter synthetic valve rests on, while a plastic washer is threaded to be flushed against the synthetic valve, which secures the valve against displacement from the flow. The length of this phantom is 20 cm, and has 30 cm of vinyl braided tubing on both ends of the phantom. The synthetic valves were labeled 0%, 50%, 75%, and 90%, which indicates degree of valve disease, and occlusion. The 0% valve has an orifice area of 2.17 cm^2, 50% is 1.40 cm^2, and 75% is 0.91 cm^2. Please see Figure 2 for pictures of the polymeric valves. The synthetic valve used in this paper is the 90% calcific valve.

The phantom was placed in a flow circuit, which starts with fluid in a flow reservoir, is pumped by a programmable physiologic pump, then to the phantom via hoses and flow connectors, and back to the reservoir. The working fluid was a blood mimicking fluid that is 60% distilled water and 40% glycerol, which results in viscosity = 0.0043 Pascal*s, density = 1035 kg/m^3 [6]. See Figure 2 for the flow circuit.

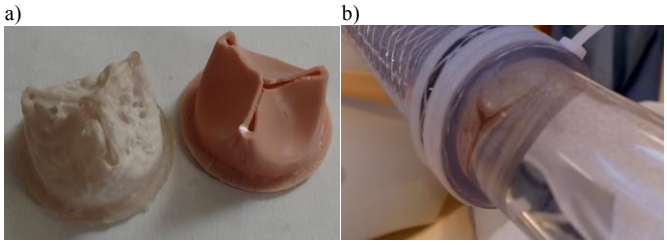

Figure 2: A) Synthetic calcific valves, at 50%(Left) and at 0% (Right) calcification. The valves, which are 1" in diameter are made of Polyurethane with various levels of calcium phosphate [10]. B) Plexiglass housing containing an interchangeable synthetic valve connected to flow circuit, pictured as meshed tubing.

C. Acquisitions

4D Flow imaging was performed on a Philips Achieva 1.5 T scanner using either a 16 element XL Torso coil or 8 element SENSE knee coil. Image acquisition was performed via both 4D Cartesian flow and 4D Spiral flow. The scan parameters for all the acquisitions are shown in Table 1. The peak flow rate is defined as the peak rate set on the pump for any steady or pulsatile flows. Qmax was set to 200 ml/s. The set peak flow for pulsatile flow experiments could not be reached because of damping of the waveform by the compliant hosing. The pump controlled the triggering frequency for the phantom, which determined the cardiac gating for these acquisitions. The Venc switch time from systolic to diastolic (T_{DV} in Figure 1) was chosen such that the peak systolic flow for a 2-D test acquisition was no longer trending negatively. The total scan time for the Cartesian acquisition was 38 minutes, while the scan time for the comparable Dual Venc Spiral acquisition resulted in 57% savings at 18 minutes.

To determine the effect of Venc on noise on both scan methods, no flow scans were also performed, where the pump flow rate was set to zero for all time (Qmax=0 mL/s). Both the conventional 4D flow and the 4D single Venc Spiral 4D flow were used to scan at Venc=200 and 40 cm/s. To ascertain noise variation in space-time, both acquisitions were gated ata triggering frequency of 60 beats per min, for 16 cardiac phases. The rest of the scan parameters were the

Table 1: Scan Parameters for the 4D Flow acquisitions

		Valve Phantom (Qmax=200 mL/s)	**Patient/Volunteer Scan**
RF Coil		SENSE Knee Coil	XL Torso Coil
Field of View (mm)		100*100*54	200*200*50
Resoultion (mm)		1.5*1.5*3	2.5*2.5*5
Matrix Size		68*68	80*80
Slices		18	10
Flip Angle (°)		8	8
Triggering Frequency (min^{-1})		40	Varies
	Number of Phases	28	16
	Systolic V_{enc} (cm/s)	350	400
	Diastolic V_{enc} (cm/s)	150	100
	T_{DV} ,V_{enc} Switch Time (ms)	450	Varies (default= 400)
Cartesian (Single or Dual Venc)	TE/TR (ms)	4.2/14	2.8/14
	Readout Time (ms)	3.4	2.1
Spiral (Single or Dual Venc)	TE/TR (ms)	1.75/14	2.3/14
	Readout Time (ms)	4	4
	Number of Interleaves	32	16

same as the Valve Phantom in Table 1 for Qmax=200 ml/s.

D. Analysis of Results

Postprocessing was started via manual segmentation in GTFlow (Gyrotools, Zurich, Switzerland) endeavoring to minimize partial flow voxels captured in the region of interest (ROI). The contours were then converted to mask images, which were used to initialize in house MATLAB (The MathWorks, Natick, MA) developed scripts. These scripts were used to compute flow waveforms, scatter plots, and velocity data characteristics. 3D visualizations, such as pathlines, vector plots, and re-sliced velocity magnitude profiles were generated in GTFlow.

The contours for no-flow data delimited the phantom boundaries – since velocity for all points should be zero – averaging the velocity in the lumen yields a measure of mean velocity error while variance of velocity values yields a measure of noise powerThis was done on a per slice basis for each of the 4D Flow acquisitions.

For the Qmax=200 data, scatter plots were used to compare the resultant net flow from related slices and times. This data was then used in conjunction with a linear fit, and Pearson correlation coefficient calculations in order to determine the similarity between performed scans. The correlation coefficient was calculated with confidence interval of 99% ($p<0.01$). The comparison was done between Dual-Venc and High Venc scans.

III. Results and Validations

A. No Flow (Qmax = 0 ml/s)

Since the pump is not active for this acquisition any measured velocities for the flow ROI can be seen as measurement noise. The average of the velocities over the ROI is the mean error, while the distribution of the velocities for each slice location and over time can be used to calculate the variance of the noise – resulting in the noise power (see figure 2). The measured error, and error standard distribution is dependent primrily on V_{enc}. Since this error does not seem to be dependent on slice, the error in Figure 3, can be combined. This means Spiral acquisition has a mean velocity error of 3.05 cm/s for Venc=200 cm/s, and 1.18 cm/s for Venc=40 cm/s. The variance of the error for these scans are 1.51 cm^2/s^2 (Venc=200 cm/s) and 0.12 cm^2/s^2 (Venc=40 cm/s). The Cartesian acquisition mean velocity and velocity variance values are very similar to the ones listed for the Spiral acquisition.

B. Pulsatile Flow (Qmax=200 mL/s)

The flow waveform for the 90% calcific valve can be seen in Figure 4. This shows the flow waveform through the valve. The flow rate seem to match quite well during peak flow rate, but differences begin to emerge during diastole. Note the significant damping – with prescribed Qmax = 200 ml/s, the measured Qmax = 90 ml/s.

Figure 5 shows a flow scatter plot comparing the measured flow for three acquisitions. The Spiral Dual-Venc acquisition against Cartesian High Venc(350 cm/s), and Cartesian Dual-Venc(350-150cm/s) (Table 1). Both fits show linear correlation with slope close to 1, however the bias is quite different between the two comparisons. The

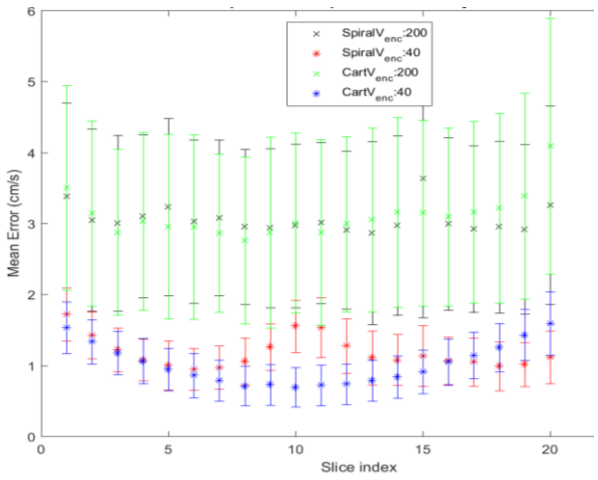

Figure 3: No Flow(Qmax=0mL/s) acquisition - lumen voxel velocities were averaged over space and all phases and displayed on a slice by slice basis. The standard distribution of the velocities over each ROI leads to the error bars. The mean error and standard deviation of error are highly dependent on V_{enc},

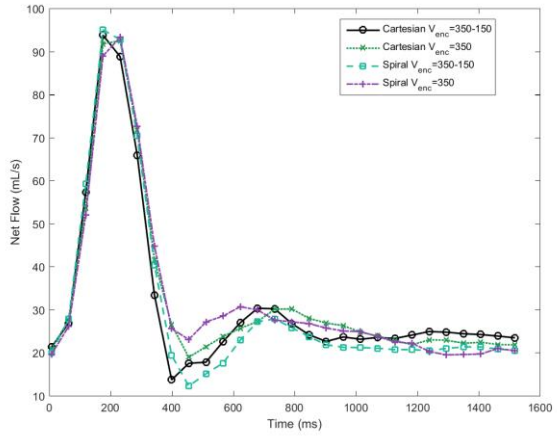

Figure 4: Flow waveform for the synthetic polymeric valve with 90% calcification. The slice location is at the valve level. The flow waveform was calculated for single High V_{enc}(350 cm/s), and the Dual-V_{enc}(350-150 cm/s) for both Spiral and Cartesian trajectories. The Dual-V_{enc} switch time was 450 ms. The R-R interval was 1500ms

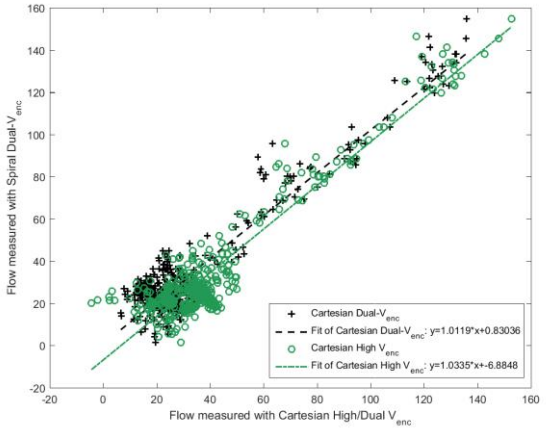

Figure 5: Flow scatter plot for the 90% calcific valve. This scatter plot compares the flow measured with Spiral Multi-Venc with Cartesian High V_{enc}(black) or Cartesian Dual-V_{enc}(green) (see table 1 for scan parameters).

a)

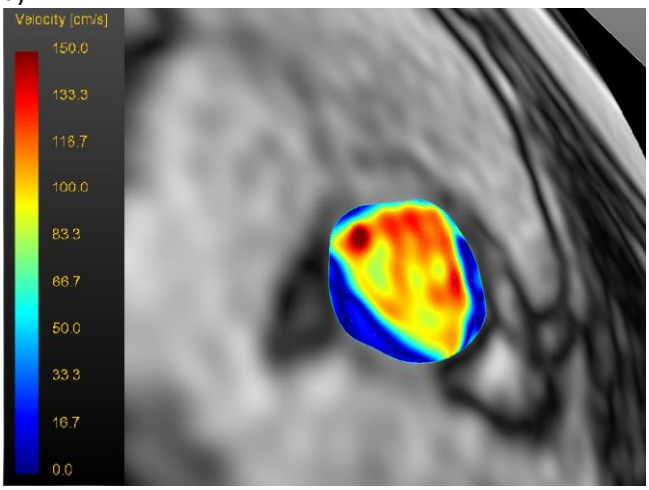

b)

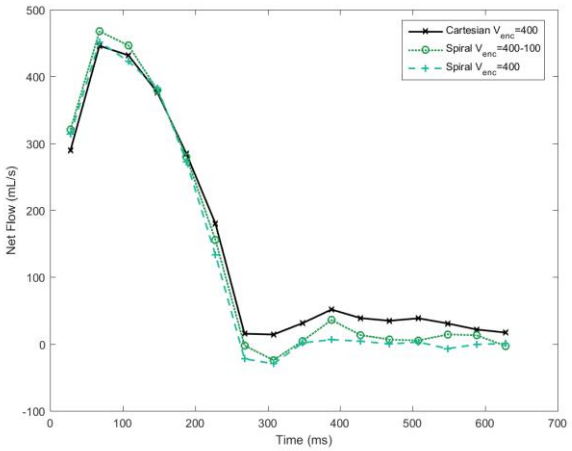

Figure 6: Results for a healthy volunteer. A) shows the velocity magnitude through a healthy volunteer's aortic valve at peak systole. B) displays the flow waveform through the valve Three scan results are shown – 4D Cartesian Flow with Venc = 400 cm/s, 4D Spiral Flow with Venc=400 cm/s and 4D Dual Venc Spiral Flow with Venc=400/100 cm/s.

Pearson correlation coefficients still show agreement with values of 0.941 when compared to Cartesian High Venc, and 0.944 when compared to Cartesian Dual-Venc.

C. Volunteer Results

The efficacy analysis was also performed on the volunteer data sets (5 volunteers), (see Table 1 and Figure 6). Figure 6a shows the velocity distribution through the valve at peak flow for a Spiral Dual-Venc scan. The Dual-Venc velocity distribution shows a slight bias, which can be seen in the net flow calculated in Figure 6b. The correlation between the Cartesian scan and the Spiral Dual-Venc was calculated, and resulted in 0.988 correlation coefficient. The Cartesian scan was correlated to Spiral single Venc, which resulted in a correlation coefficient 0.986.

IV. Conclusion

A temporally variant 4D Dual-Venc Spiral flow acquisition was designed, implemented, and tested. Relative to 4D Cartesian flow, Spiral Dual-Venc has the advantage of a shorter TE, which reduces flow artifacts and intravoxel dephasing. Spiral Dual-Venc acquisitions also maintains the advantage of decreasing the scan time in comparison the Cartesian acquisitions.

The results also show the Dual-Venc acquisition to have comparable flow measurement accuracy to Cartesian and Spiral single Venc acquisitions. What should be kept in mind however is that any measurement requiring data processing and computation of derivatives or visualization such as generation of pathlines, measurement of pressures [11] or wall shear stress from the 4D flow data will necessarily be more accurate with the dual Venc acquisition because of increased SNR and VNR in the diastolic phase of the dual Venc data. We are confident that future results in patients with aortic stenosis will show the additional power of this method.

Acknowledgment

This research has been supported by NIH Grant R21HL132263

References

[1] M. Markl, A. Frydrychowicz, S. Kozerke, M. Hope and O. Wieben, "4D flow MRI," *Journal of Magnetic Resonance Imaging,* vol. 36, no. 5, pp. 1015-1036, 2012.

[2] T. Sekine, Y. Amano, R. Takagi, Y. Matsumura, Y. Murai and S. Kumita, "Feasibility of 4D flow MR imaging of the brain with either Cartesian yz radial sampling or kt SENSE: comparison with 4D flow MR imaging using SENSE," *Magnetic Resonance in Medical Sciences,* vol. 13, no. 1, pp. 15-24, 2014.

[3] F. Huang, J. Akao, S. Vijayakumar, G. R. Duensing and M. Limkeman, "k-t GRAPPA: A k-space implementation for dynamic MRI with high reduction factor," *Magnetic Resonance in Medicine,* vol. 54, no. 5, pp. 1172-1184, 2005.

[4] M. Lustig, D. Donoho and J. M. Pauly, "Sparse MRI: The application of compressed sensing for rapid MR imaging," *Magnetic resonance in medicine,* vol. 58, no. 6, pp. 1182-1195, 2007.

[5] M. Kadbi, M. Negahdar, M. Traughber, P. Martin, M. F. Stoddard and A. A. Amini, "4D UTE flow: a phase-contrast MRI technique for assessment and visualization of stenotic flows," *Magnetic resonance in medicine,* vol. 73, no. 3, pp. 939-950, 2015.

[6] M. Negahdar, M. Kadbi, M. Kendrick, M. F. Stoddard and A. A. Amini, "4D spiral imaging of flows in stenotic phantoms and subjects with aortic stenosis," *Magnetic resonance in medicine,* vol. 75, no. 3, pp. 1018--1029, 2016.

[7] N. J. Pelc, M. A. Bernstein, A. Shimakawa and G. H. Glover, "Encoding strategies for three-direction phase-contrast MR imaging of flow," *Journal of Magnetic Resonance Imaging,* vol. 1, no. 4, pp. 405--413, 1991.

[8] H. Ha, G. B. Kim, J. Kweon, Y.-H. Kim, N. Kim, D. H. Yang and S. J. Lee, "Multi-VENC acquisition of four-dimensional phase-contrast MRI to improve precision of velocity field measurement," *Magnetic Resonance in Medicine,* 2015.

[9] S. Schnell, S. A. Ansari, C. Wu, J. Garcia, I. G. Murphy, O. A. Rahman, A. A. Rahsepar, M. Aristova, J. D. Collins, J. C. Carr and M. Markl, "Accelerated dual-venc 4D flow MRI for neurovascular applications," *Journal of Magnetic Resonance Imaging,* 2017.

[10] A. Falahatpisheh, D. Morisawa, T. T. Toosky and A. Kheradvar, "A calcified polymeric valve for valve-in-valve applications," *Journal of Biomechanics Vol.50,* pp. 77--82, 2017.

[11] A. Nasiraei-Moghaddam, G. Behrens, N. Fatouraee, R. Agarwal, E. T. Choi and A. A. Amini, "Factors affecting the accuracy of pressure measurements in vascular stenoses from phase-contrast MRI," *Magnetic resonance in medicine,* vol. 52, no. 2, pp. 300-309, 2004.